PHYSICAL REVIEW E **77**, 035701(R) (2008)

Thermal lattice Boltzmann model for gases with internal degrees of freedom

Xiaobo Nie, Xiaowen Shan, and Hudong Chen
Exa Corporation, 3 Burlington Woods Drive, Burlington, Massachusetts 01803, USA
(Received 2 July 2007; revised manuscript received 29 October 2007; published 17 March 2008)

We rigorously derive a dramatically simplified kinetic model for fluids with internal degrees of freedom. With proper discretization in velocity space, the model leads to a lattice Boltzmann model for polyatomic gases. The macroscopic recovery of correct hydrodynamics is theoretically shown and numerically validated.

DOI: 10.1103/PhysRevE.77.035701 PACS number(s): 47.11.Qr, 47.40.−x, 47.45.Ab, 47.10.ad

In recent years, as an alternative method of computational fluid dynamics (CFD), the lattice Boltzmann (LB) method has attracted substantial amount of attention [1–3]. The uniqueness of this method is its root in kinetic theory which gives it several critical advantages in modeling microflows [4,5], flows in complex geometries [6,7] and multicomponent and multiphase fluid systems [8,9]. In addition, the explicit and local interaction makes it easy for parallel realizations in large scale simulations.

The LB method originated from the lattice gas cellular automaton [10,11]. The single-relaxation-time (BGK [12]) collision model was adopted. In the early development the equilibrium distribution function is chosen to be a small-Mach number expansion containing a few coefficients. These coefficients are then determined using the requirement that the macroscopic equations obtained through Chapman-Enskog calculation agree with the Navier-Stokes equations [13,14]. This approach has achieved great success in devising LB models for the continuity and momentum equations. However the effort of recovering the energy equation [15–17] has met some difficulties due to numerical instability [18,19]. Although it has been known that increasing the set of velocities will improve the stability, no criterion was known at that time to determine the additional velocities.

Recently, the LB method was given a new theoretical interpretation as a moment solution of the BGK equation using the Hermite polynomials as the expansion basis [20,21]. The equilibrium distribution function in the discrete model is obtained by truncating the Hermite expansion of the Maxwellian distribution. It was further shown that the correct hydrodynamic equations are guaranteed by the kinetic equation as long as sufficient number of moments are preserved by the truncation and accurately represented by the discrete velocities [21]. Specifically, the energy equation at the Navier-Stokes level is approximately recovered up to a small error in the thermal diffusivity if the third moments of the Maxwellian are preserved. It is exactly recovered if the fourth order moments are preserved. This way, thermal LB models can be constructed without using the small-Mach number condition.

In this derivation, and in most other thermal LB models as well, the gas molecules are assumed to be monatomic, yielding most noticeablly a fixed specific heat ratio. In reality, a polyatomic gas may have a specific heat ratio varying from 1.2 to 5/3 [22]. Therefore it is important for any practical computational scheme for compressible flows to be able to handle a variable specific heat ratio. There are a few LB models with variable specific heat ratio in some specific conditions. Most of them aim to simulate Euler equations [23–27]. The two-dimensional Navier-Stokes equations are recovered in Ref. [25] by the finite difference LB method with a small time step.

In this paper, we propose a general approach for treating the effect of the internal degrees of freedom of the polyatomic gas molecules to the equations of conservative quantities. In this approach we rigorously derived a dramatically simplified Boltzmann equation. This simplification can be applied to any other kinetic approaches if only moments of conservative quantities are of interest. As one direct application of the result, a LB model with a variable ratio of specific heat is obtained. The conservation equations of mass, momentum and energy derived by a Chapman-Enskog expansion recover the complete Navier-Stokes equations of polyatomic gas for any dimension. The theoretic results have been validated by simulating sound waves, heat transfer, and the Sod-Riemann problem.

The classic kinetic theory treatment of gases with internal degrees of freedom is rather standard. Consider a gas consisting of molecules with S internal degrees of freedom. Let $\boldsymbol{x}$ and $\boldsymbol{\xi}$ be the coordinates and translational velocity in a conventional D-dimensional space, q_i, $\zeta_i \equiv \dot{q}_i$ and I_i, $i=1,\ldots,S$, the general coordinates, velocities, and inertia of the internal degrees of freedom, respectively. The Hamiltonian is

$$H(\boldsymbol{\xi},\boldsymbol{\zeta}) = \frac{1}{2}\left(m\xi^2 + \sum_{i=1}^{S} I_i\zeta_i^2\right). \tag{1}$$

The single-particle distribution function is now a $2(D+S)$ dimensional function. We ignore the variations in the S dimensions spanned by the coordinates q_i and write $f=f(\boldsymbol{\xi},\boldsymbol{\zeta},\boldsymbol{x},t)$. As usual, the density ρ, fluid velocity $\boldsymbol{u}$, and internal energy density per mass ϵ, are the moments of f:

$$\rho = m\int f d\boldsymbol{\xi} d\boldsymbol{\zeta}, \tag{2a}$$

$$\rho\boldsymbol{u} = m\int f\boldsymbol{\xi} d\boldsymbol{\xi} d\boldsymbol{\zeta}, \tag{2b}$$

$$\rho\epsilon = \frac{m}{2}\int f|\boldsymbol{\xi}-\boldsymbol{u}|^2 d\boldsymbol{\xi} d\boldsymbol{\zeta} + \frac{1}{2}\int f\sum_{i=1}^{S} I_i\zeta_i^2 d\boldsymbol{\xi} d\boldsymbol{\zeta}. \tag{2c}$$

Let the evolution of f in $\boldsymbol{x}$ space be governed by the following Boltzmann equation with a BGK collision model:

$$\frac{\partial f}{\partial t} + \boldsymbol{\xi}\nabla f = -\frac{1}{\tau}[f - f^{(\mathrm{eq})}]. \tag{3}$$

Hereinafter, we adopt the same dimensionless units of Ref. [21]. The equilibrium distribution function $f^{(\mathrm{eq})}$ is [22]

$$f^{(\mathrm{eq})} = nZ^{-1}\exp\left[-\frac{m|\boldsymbol{\xi}-\boldsymbol{u}|^2 + \sum_{i=1}^{S} I_i\zeta_i^2}{2\theta}\right]. \tag{4}$$

where $n=n(\boldsymbol{x},t)$ is the number density, θ the temperature, and Z the partition function:

$$Z = \left(\frac{m}{2\pi\theta}\right)^{-D/2}\prod_{i=1}^{S}\left(\frac{I_i}{2\pi\theta}\right)^{-1/2}. \tag{5}$$

Substituting Eqs. (4) and (5) into Eq. (2c), we identify the internal energy as

$$\epsilon = \frac{1}{2}(D+S)\theta, \tag{6}$$

which yields the specific heat ratio of

$$\gamma = \frac{D+S+2}{D+S}. \tag{7}$$

By examining Eqs. (2)–(5), it is found that the dynamics of $(2D+S)$-dimensional f can be described by two loosely coupled $(2D)$-dimensional distributions. The two reduced distribution functions are moments of f in $\boldsymbol{\zeta}$ space:

$$g_1(\boldsymbol{\xi}) = \int f(\boldsymbol{\xi},\boldsymbol{\zeta})d\boldsymbol{\zeta}, \tag{8a}$$

$$g_2(\boldsymbol{\xi}) = \frac{1}{S}\sum_{i=1}^{S} I_i \int \zeta_i^2 f(\boldsymbol{\xi},\boldsymbol{\zeta})d\boldsymbol{\zeta}, \tag{8b}$$

Eqs. (2) reduce to a form very close to their counterparts for monatomic gases

$$\rho = m\int g_1 d\boldsymbol{\xi}, \tag{9a}$$

$$\rho\boldsymbol{u} = m\int g_1\boldsymbol{\xi}d\boldsymbol{\xi}, \tag{9b}$$

$$\rho\epsilon = \frac{m}{2}\int g_1|\boldsymbol{\xi}-\boldsymbol{u}|^2 d\boldsymbol{\xi} + \frac{S}{2}\int g_2 d\boldsymbol{\xi}. \tag{9c}$$

The dynamic equations for g_1 and g_2 can be obtained by taking the same two moments of Eq. (3). Noticing that $f^{(\mathrm{eq})}$ can be written as the product of Maxwellians in separate variables, we arrive at

$$\frac{\partial g_i}{\partial t} + \boldsymbol{\xi}\cdot\nabla g_i = -\frac{1}{\tau}[g_i - g^{(\mathrm{eq})}h_i], \quad i=1,2, \tag{10}$$

where $g^{(\mathrm{eq})}$ is the Maxwellian for translational motion

$$g^{(\mathrm{eq})} = n\left(\frac{m}{2\pi\theta}\right)^{D/2}\exp\left[-\frac{m|\boldsymbol{\xi}-\boldsymbol{u}|^2}{2\theta}\right] \tag{11}$$

and

$$h_1 \equiv \int g_i(\zeta_i)d\zeta_i = 1, \tag{12a}$$

$$h_2 \equiv \frac{1}{S}\sum_{i=1}^{S} I_i \int \zeta_i^2 \prod_{i=1}^{S} g_i(\zeta_i)d\zeta_i = \theta. \tag{12b}$$

Equations (9)–(12) and (6) are the kinetic equations which model the hydrodynamics of a gas with internal degrees of freedom. Except for the last term of in Eq. (9c) representing energy exchange with the internal motion, the equation for g_1 is identical to the monatomic BGK equation. The temperature is now given by Eqs. (6) and (9c), which depend on the dynamics of g_2. It is also noticed that S just represents the coupling strength between the two reduced distribution functions and is not necessary to be an integer anymore.

The discrete velocities of the LB model for a polyatomic gas can be constructed using any Hermite quadrature accurate enough to recover the energy equation [21]. The left side of Eq. (10) can be discretized using the first upwind scheme and taking $\delta x_a = \xi_a\delta_t$. Here δx and δ_t are spatial and time steps, respectively. The discrete LB equation can be written as

$$g_{i,a}(\mathbf{x}+\boldsymbol{\xi}_a\delta_t, t+\delta_t) - g_{i,a}(\mathbf{x},t) = -\frac{1}{\tau}[g_{i,a} - g_{i,a}^{(\mathrm{eq})}h_i]. \tag{13}$$

Here a indicates the discrete velocities. The equilibrium distribution is

$$\begin{aligned} g_{i,a}^{(\mathrm{eq})} = w_a\rho\Bigg(& 1 + \boldsymbol{\xi}_{a\alpha}u_\alpha + \frac{1}{2}[(\boldsymbol{\xi}_{a\alpha}u_{a\alpha})^2 - u^2] \\ &+ \frac{\theta-1}{2}(\boldsymbol{\xi}_a^2 - D) + \frac{\boldsymbol{\xi}_{a\alpha}u_\alpha}{6}[(\boldsymbol{\xi}_{a\alpha}u_{a\alpha})^2 - 3u^2] \\ &+ \frac{\theta-1}{2}(\boldsymbol{\xi}_{a\alpha}u_\alpha)(\boldsymbol{\xi}_a^2 - D - 2) \\ &+ \frac{1}{24}[(\boldsymbol{\xi}_{a\alpha}u_\alpha)^4 - 6(\boldsymbol{\xi}_{a\alpha}u_\alpha)^2u^2 + 3u^4] \\ &+ \frac{\theta-1}{4}\{(\boldsymbol{\xi}_a^2 - D - 2)[(\boldsymbol{\xi}_{a\alpha}u_\alpha)^2 - u^2] - 2(\boldsymbol{\xi}_{a\alpha}u_\alpha)^2\} \\ &+ \frac{(\theta-1)^2}{8}[\boldsymbol{\xi}_a^4 - 2(D+2)\boldsymbol{\xi}_a^2 + D(D+2)]\Bigg). \end{aligned} \tag{14}$$

Following the standard procedure to derive hydrodynamic equations [13,14,22,28], we use a Chapman-Enskog expansion to obtain the conservation equations of mass, momentum, and energy:

$$\partial_t\rho + \partial_\alpha(\rho u_\alpha) = 0, \tag{15a}$$

$$\partial_t(\rho u_\alpha) + \partial_\beta(\rho u_\alpha u_\beta) + \partial_\beta P_{\alpha\beta} = 0, \tag{15b}$$

TABLE I. The abscissas and weights of a ninth-order accurate Gauss-Hermite quadrature formula in three dimensions. Here p is the number of abscissas in the symmetry class and r is the lattice constant. The subscript "FS" denotes fully symmetric permutations.

ξ_a	p	w_a
$(0,0,0)$	1	$3.05916220294860\times10^{-2}$
$(r,0,0)_{\mathrm{FS}}$	6	$9.85159510372633\times10^{-2}$
$(\pm r,\pm r,\pm r)$	8	$2.75250053256381\times10^{-2}$
$(2r,r,0)_{\mathrm{FS}}$	24	$6.11102336683342\times10^{-3}$
$(2r,2r,0)_{\mathrm{FS}}$	12	$4.28183593681084\times10^{-4}$
$(3r,0,0)_{\mathrm{FS}}$	6	$3.24747527088073\times10^{-4}$
$(3r,2r,0)_{\mathrm{FS}}$	24	$1.43186241154802\times10^{-5}$
$(\pm2r,\pm2r,\pm2r)$	8	$1.81021751576374\times10^{-4}$
$(3r,r,r)_{\mathrm{FS}}$	24	$1.06834002459391\times10^{-4}$
$(\pm3r,\pm3r,\pm3r)$	8	$6.92875089638602\times10^{-7}$
		$r=1.19697977039307$

$$\partial_t(\rho\epsilon)+\partial_\alpha(\rho\epsilon u_\alpha)+P_{\alpha\beta}\partial_\alpha u_\beta+\partial_\alpha q_\alpha=0, \tag{15c}$$

where

$$P_{\alpha\beta}=p\delta_{\alpha\beta}-\rho\nu\left[(\partial_\alpha u_\beta+\partial_\beta u_\alpha)-\frac{2}{D}\delta_{\alpha\beta}\partial_\gamma u_\gamma\right]-\rho\eta\delta_{\alpha\beta}\partial_\gamma u_\gamma, \tag{16a}$$

$$q_\alpha=-\rho\kappa\frac{D+S+2}{2}\partial_\alpha\theta, \tag{16b}$$

where $p=\rho\theta$ defines the ideal gas equation of state, and ν, η, and κ are the shear viscosity, the volume viscosity, and the thermal diffusivity, respectively,

$$\nu=\kappa=\left(\tau-\frac{1}{2}\right)\theta\delta_t \quad \text{and} \quad \eta=\frac{2S\nu}{D(D+S)}. \tag{17}$$

Macroscopically, the introduction of additional degrees of freedom causes a nonzero volume viscosity in addition to changing the heat capacities.

In the rest of this paper we present numerical validations using a three-dimensional ninth-order accurate quadrature employing 121 velocities. A two-dimensional projection of this model was used in the previous study of linear hydrodynamic waves [29]. The abscissas and weights are given in Table I. It is worth pointing out that the equilibrium distribution that is the fourth-order Hermite expansion of the Maxwellian and the velocity abscissas with the ninth-order quadrature together ensure that the Navier-Stokes thermodynamics is recovered with full Galilean invariance [21].

We first measure the specific heat ratio through the sound speed $c_s=\sqrt{\gamma\theta}$, which is in turn measured through the oscillation frequency of a standing sound wave. We performed the simulation with two different relaxation times and for cases in which the wave vector $\boldsymbol{k}$ is aligned with the primary lattice links and the diagonals respectively. In lattice units, the simulation domain size is $100\times1\times1$ for the case of sound wave traveling in the x direction, and $100\times100\times1$ for the case of sound wave traveling in the diagonal direction. The numerical measurement of γ agrees very well with the theoretic prediction as shown in Fig. 1. For most gases, the specific heat ratio varies from 1.2 to 5/3 [22], corresponding to S from about 10 to 0. The case of $S\to\infty$ ($\gamma\to1$) corresponds to the isothermal process whereas $S=0$ ($\gamma=5/3$) corresponds to a monatomic gas. As shown in Fig. 1, even for negative S up to $S=-2$, the LB model still gives correct γ. Although no such gas exists in reality, the capability of simulating such high γ value may have potential application somewhere else.

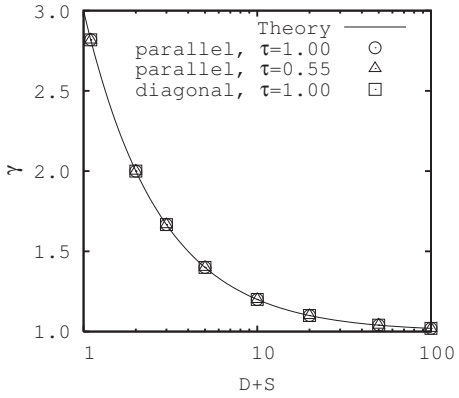

FIG. 1. The specific heat ratio γ obtained from measuring sound speed as a function of total dimension $D+S$. The solid line represents the Chapman-Enskog result (7). The circles and triangles stand for the sound waves traveling in the x direction with different relaxation times $\tau=1$ and $\tau=0.55$, respectively. The squares are for $\tau=1$ in the sound waves traveling in the diagonal direction of the lattice.

The second numerical experiment is designed to directly validate the thermal diffusivity. The simulation domain size is $64\times1\times1$ with periodic boundary conditions applied in all directions. At each time step, the same amount of heat $\frac{D+S}{2}\rho\delta\theta$ is injected at $x=1$ and removed at $x=32$ by adding and subtracting $\delta\theta$ to the post-advection temperature used to obtain the new equilibrium distributions. When the temperature becomes steady, a linear spatial profile of temperature is observed between the two points. From Eqs. (15c) and (16b), the derivative of temperature is given by

$$\frac{d\theta}{dx}=\frac{D+S}{2\kappa(D+S+2)}\frac{\delta\theta}{\delta_t}. \tag{18}$$

Excellent agreement between the simulation and the theoretical result above is found as shown in Fig. 2. The thermal diffusivity of the LB fluid has indeed been affected by the additional degrees of freedom as expected.

The last numerical experiment is the one-dimensional Sod-Riemann problem [30]. Initially the gas is at different states on the two sides of the middle point, i.e., for $x/L\le\frac{1}{2}$, $\rho=1$, $u=0$, and $p=1$, and for $x/L>\frac{1}{2}$, $\rho=0.1$, $u=0$, and $p=0.125$. Here $L=1000$ is the length of the domain. The solution at $t=200\delta_t$ is shown in Fig. 3. A rarefaction wave at left, a shock at right and a contact discontinuity at middle are observed. In terms of constant regions and positions of discontinuity, the numerical solution agrees very well with the

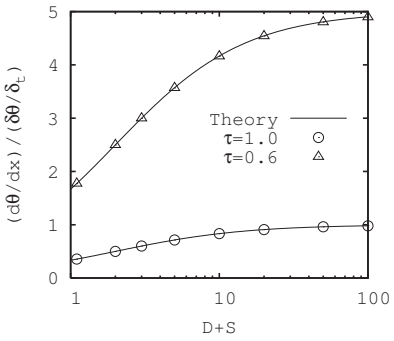

FIG. 2. The derivative of temperature as a function of total dimensions $D+S$. The solid line represents the Chapman-Enskog result (18). The circles and triangles stand for numerical results with different relaxation times $\tau=1$ and $\tau=0.6$, respectively.

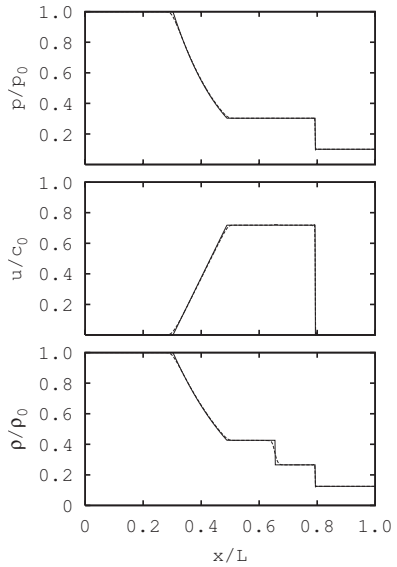

FIG. 3. The profiles of pressure p, velocity u and density ρ at $t=200\delta_t$, i.e., $t=0.163L/c_0$ in the Sod-Riemann solution. Here p_0, c_0, and ρ_0, respectively, are initial pressure, sound speed, and density on the left side of the simulation domain. The ratio of specific heat $\gamma=1.4$. The relaxation time $\tau=0.75$.

theoretic solution for ideal gas, i.e., with zero viscosity and heat diffusivity. The smooth effect at the contact discontinuity and the two ends of the rarefaction wave in the numerical solution results from finite viscosity and heat diffusivity. When the viscosity and the heat diffusivity are reduced, the contact discontinuity will become sharper. However, oscillations start to appear near the shock. This kind of oscillation is a well-known numerical artifact due to insufficient numerical resolution in general.

In summary, we have rigorously derived a discrete kinetic model for gases with internal degrees of freedom based on the Boltzmann equation and the generalized Maxwellian distribution. The model is shown both analytically and numerically to recover the complete Navier-Stokes equations of a polyatomic gas. It will allow the LB method to be applied to a more general class of problems of compressible fluid flows.

This work was supported in part by the National Science Foundation.

[1] S. Chen and G. Doolen, Annu. Rev. Fluid Mech. **30**, 329 (1998).
[2] S. Succi, *The Lattice Boltzmann Equation for Fluid Dynamics and Beyond, Numerical Mathematics and Scientific Computation* (Oxford University Press, Oxford, 2001).
[3] H. Chen, S. Kandasamy, S. Orszag, R. Shock, S. Succi, and V. Yakhot, Science **301**, 633 (2003).
[4] X. B. Nie, G. D. Doolen, and S. Chen, J. Stat. Phys. **107**, 279 (2002).
[5] F. Toschi and S. Succi, Europhys. Lett. **69**, 549 (2005).
[6] N. S. Martys and H. Chen, Phys. Rev. E **53**, 743 (1996).
[7] X. B. Nie and N. S. Martys, Phys. Fluids **19**, 011702 (2007).
[8] X. Shan and H. Chen, Phys. Rev. E **47**, 1815 (1993).
[9] X. B. Nie, Y.-H. Qian, G. D. Doolen, and S. Chen, Phys. Rev. E **58**, 6861 (1998).
[10] U. Frisch, B. Hasslacher, and Y. Pomeau, Phys. Rev. Lett. **56**, 1505 (1986).
[11] S. Wolfram, J. Stat. Phys. **45**, 471 (1986).
[12] P. L. Bhatnagar, E. P. Gross, and M. Krook, Phys. Rev. **94**, 511 (1954).
[13] H. Chen, S. Chen, and W. H. Matthaeus, Phys. Rev. A **45**, R5339 (1992).
[14] Y. H. Qian, D. d'Humieres, and P. Lallemand, Europhys. Lett. **17**, 479 (1992).
[15] F. J. Alexander, H. Chen, S. Chen, and G. D. Doolen, Phys. Rev. A **46**, 1967 (1992).
[16] Y. Chen, H. Ohashi, and M. Akiyama, Phys. Rev. E **50**, 2776 (1994).
[17] H. Chen, C. Teixeira, and K. Molvig, Int. J. Mod. Phys. C **8**, 675 (1997).
[18] G. R. McNamara, A. L. Garcia, and B. J. Alder, J. Stat. Phys. **81**, 395 (1995).
[19] G. R. McNamara, A. L. Garcia, and B. J. Alder, J. Stat. Phys. **87**, 1111 (1997).
[20] X. Shan and X. He, Phys. Rev. Lett. **80**, 65 (1998).
[21] X. Shan, X.-F. Yuan, and H. Chen, J. Fluid Mech. **550**, 413 (2006).
[22] S. Chapman and T. G. Cowling, *The Mathematical Theory of Non-Uniform Gases*, 3rd ed. (Cambridge University Press, London, 1970).
[23] J. Huang, F. Xu, M. Vallières, D. H. Feng, Y.-H. Qian, B. Fryxell, and M. R. Strayer, Int. J. Mod. Phys. C **8**, 827 (1997).
[24] C. Sun and A. T. Hsu, Phys. Rev. E **68**, 016303 (2003).
[25] M. Watari, Physica A **382**, 502 (2007).
[26] Guangwu Yan, Yaosong Che, and Hu Shouxin, Phys. Rev. E **59**, 454 (1999).
[27] T. Kataoka and M. Tsutahara, Phys. Rev. E **69**, 056702 (2004).
[28] C. Cercignani, *Theory and Application of the Boltzmann Equation* (Plenum, New York, 1990).
[29] X. Shan and H. Chen, Int. J. Mod. Phys. C **18**, 635 (2007).
[30] G. Sod, J. Comput. Phys. **27**, 1 (1978).